Final-State Interaction Effects in Weak Three-Body Decays*

R. D. AMADO AND J. V. NOBLE

Department of Physics, University of Pennsylvania, Philadelphia, Pennsylvania 19104

(Received 17 April 1969)

An exactly soluble model of the weak decay of a 0^+ particle to three strongly interacting 0^+ decay products is investigated numerically in order to explore the effects of final-state interactions (FSI) on the decay and the way in which the resonant-pair interaction information is distributed over the three-body final state. We find that moderately strong attractive pairwise FSI can produce very large enhancements or de-enhancements in the decay rate, but we find no effect of rescattering singularities. We find that large effects on the decay rate can be accompanied by pure phase-space single-particle spectra. The effects of interference between various terms in the amplitude make the extraction of pair-resonance parameters from singles spectra chancy, and there is no obvious trend in the deviation from the input resonance parameters. These interference effects also produce striking and possibly misleading patterns in the Dalitz plots.

I. INTRODUCTION

THREE-BODY final states occur frequently in particle and nuclear physics. In fact, many two-body systems have been studied only by means of such final states. Despite this, theoretical understanding of three-hadron states and of how two-body information is distributed over them remains at a primitive level. Currently the most widely used method of analysis is some form of Fermi-Watson theory, which singles out the interactions of a particular pair.[1] The inadequacies of this method are illustrated by the difficulty of extracting a unique set of ρ-meson parameters, or that of determining the neutron-neutron scattering length.[2,3]

This paper is a modest attempt to increase our understanding of three-hadron states by examining a simple, exactly soluble model. Since we approached the problem with almost no intuition, we restricted ourselves to the simplest possible nontrivial model. Even this problem contains a surprisingly wide range of dynamics and, as we shall see, sheds considerable light on the behavior of resonant final-state interactions. The model we studied describes the decay of a 0^+ particle (the G) into three identical 0^+ decay products (the H's). The decay is weak in the sense that the interaction producing it is treated in first order, whereas the decay products interact strongly. Thus, to treat the decay, we must solve the strong-interaction dynamics of the $3H$ system exactly. To simplify this problem we assume nonrelativistic kinematics and separable S-wave interactions. A functional form is chosen for this interaction which is capable of producing H-H resonances. As is by now well known, the separable form is appropriate to a resonance-dominated two-body scattering amplitude, and also greatly facilitates the calculation.[4]

There have been a number of previous attempts to deal with three-body decays and related problems.[5] Most have concentrated on the problem of overlapping resonances, and were motivated by perturbation-theoretical arguments. Analysis of various static models[6,7] and, more recently, a general treatment by Schmid[8] have greatly clarified some of the outstanding questions. Additionally, several authors have performed exact calculations involving three-body final states, designed to treat particular physical systems rather than to explore the range of possible phenomena.[3,9] We are aware of only one previous exploration similar in spirit and motivation to our own, that of Aitchison.[10] He solves a linear three-body formalism which, although motivated by on-shell, relativistic considerations, is in fact of the (off-shell) Faddeev form. Unfortunately, his Breit-Wigner approximations to the two-body amplitudes appearing in these equations neither satisfy off-shell two-body unitarity nor do they have the correct analytic properties. As Lovelace has emphasized,[11] these properties are essential to making the on-shell solution of the three-body problem satisfy appropriate unitary relations.

In Sec. II, we describe the model in more detail. Section II A outlines the three-body dynamical equations, Sec. II B gives the details of two-body interaction, and Sec. II C sketches the method of solution. We present our results in Sec. III. We have calculated total rates, singles spectra, and Dalitz plots which we present and discuss in Secs. III A, III B, and III C, respectively.[12] Finally, in Sec. IV we present our con-

[1] M. L. Goldberger and K. M. Watson, *Collision Theory* (John Wiley & Sons, Inc., New York, 1964), p. 540.

[2] Cf. N. Barash-Schmidt, A. Barbaro-Galtieri, L. R. Price, A. H. Rosenfeld, P. Söding, C. G. Wohl, M. Roos, and G. Conforto, Rev. Mod. Phys. 41, 109 (1969).

[3] R. Aaron and R. D. Amado, Phys. Rev. 150, 857 (1966).

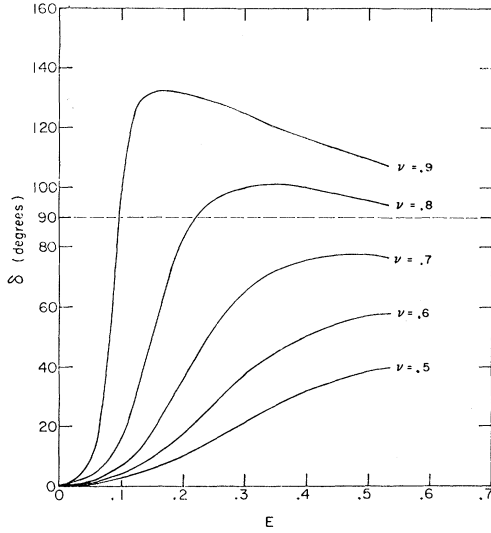[4] K. M. Watson and J. Nuttall, *Topics in Several Particle Dynamics* (Holden-Day, Inc., San Francisco, 1967).

[5] R. N. Choudhuri, Phys. Rev. 175, 2066 (1968); B. Dutta-Roy and I. R. Lapidus, *ibid.* 169, 1357 (1968); M. Parkinson, *ibid.* 172, 1607 (1968); I. J. R. Aitchison and C. Kacser, *ibid.* 173, 1700 (1968); A. Ahmadzadeh and J. A. Tjon, *ibid.* 139, B1085 (1965).

[6] C. Goebel, Phys. Rev. Letters 13, 143 (1964).

[7] F. S. Chen-Cheung and C. M. Sommerfield, Phys. Rev. 152, 1401 (1966).

[8] C. Schmid, Phys. Rev. 154, 1363 (1967).

[9] R. L. Schult and I. M. Barbour, Phys. Rev. 164, 1791 (1967); J. H. Hetherington and L. H. Schick, *ibid.* 156, 1647 (1967).

[10] I. J. R. Aitchison, Nuovo Cimento 51A, 249 (1967); See also I. Duck and F. C. Khanna, Nucl. Phys. 77, 609 (1966).

[11] C. Lovelace, Phys. Rev. 135, B1225 (1964).

[12] The results on total rates were previously reported by us; see R. D. Amado and J. V. Noble, Phys. Rev. Letters 21, 1846 (1968).

FIG. 1. Two-body $(H\text{-}H)$ phase shifts as a function of energy, for various values of the $H\text{-}H$ coupling strength ν. The units of E and ν are described in the text, below Eqs. (8) and (9).

clusions, plans for future studies, and speculate on the possible relevance of these results to actual physical systems.

II. DESCRIPTION OF MODEL

A. Three-Body Equations

The weak decay amplitude for $G \to 3H$ may be written (to all orders in the strong interactions)

$$M = \langle \psi_{3H} | \mathcal{3C}_{\text{weak}} | G \rangle, \qquad (1)$$

where the interacting state of 3 H's, $\langle \psi_{3H} |$, is defined in terms of the plane-wave state $\langle 3H |$ and the three-body T-matrix T_{3H} by

$$\langle \psi_{3H} | = \langle 3H | + \langle 3H | T_{3H}(E)G_0(E). \qquad (2)$$

Here E is the total energy release in the decay and G_0 is the free Green's function $(E - H_0)^{-1}$. The T matrix may be decomposed, following Faddeev,[13] into the sum of three terms

$$T_{3H}(E) = \sum_{\alpha=1}^{3} X_\alpha(E). \qquad (3)$$

The partial amplitudes X_α satisfy the Faddeev equations

$$X_\alpha(E) = t_\alpha(E) + t_\alpha(E)G_0(E) \sum_{\beta \neq \alpha} X_\beta(E). \qquad (4)$$

We follow the usual cyclic labeling convention where, for example, $t_1(E)$ is the fully off-shell two-body scattering amplitude for particles 2 and 3. We see from Eqs. (1) and (2) that we need to know only the following

matrix element of the X_α's:

$$\langle \mathbf{p}_\alpha, \mathbf{q}_\alpha | X_\alpha(E)G_0(E)\mathcal{3C}_{\text{weak}} | G \rangle. \qquad (5)$$

This is a certain function of the energy E, of the momentum $\mathbf{p}_\alpha$ of the particle α, and of $\mathbf{q}_\alpha$, the momentum conjugate to the relative coordinate of the α pair [i.e., $\mathbf{q}_1 = \frac{1}{2}(\mathbf{p}_2 - \mathbf{p}_3)$]. Because of the identity of the H particles (they have no internal quantum numbers), the entire dependence of the matrix element in Eq. (5) on the particle label α is carried by $\mathbf{p}_\alpha$ and $\mathbf{q}_\alpha$, so that we can drop the α label on X. That is, X_α is the same function of its special variables as X_β is of its.

B. Two-Body Interaction

The fully off-shell two-body t matrix appearing in Eq. (4) is taken to have the separable form

$$\langle \mathbf{p}_\alpha, \mathbf{q}_\alpha | t_\alpha(E) | \mathbf{p}_\alpha', \mathbf{q}_\alpha' \rangle$$
$$= \delta(\mathbf{p}_\alpha - \mathbf{p}_\alpha')v(q_\alpha^2)\tau(E - (3/4M_H)p_\alpha^2)v(q_\alpha'^2), \qquad (6)$$

where M_H is the mass of the H, and $v(q^2)$ is the vertex function of the interaction. In terms of this vertex function, the function τ of Eq. (6) is

$$\tau(E) = -\left[\lambda^{-1} + \int d\mathbf{q} \frac{v^2(q^2)}{E - q^2/M} \right]^{-1}, \qquad (7)$$

where λ is the two-body coupling constant. Equation (7) may be obtained, for example, by insisting that Eq. (6) satisfy off-shell two-body unitarity.[14] This condition is essential in order that Eq. (4) yield a unitary three-body amplitude.[11] We wish to study a case in which the two-body subsystem can resonate: The vertex function $v(q^2)$ was chosen to satisfy this requirement as well as to facilitate the numerical analysis. To avoid the complications (which we believe are inessential for the physics) of higher spins, we have chosen the $H\text{-}H$ interaction Eq. (6) to act only in S waves. A $v(q^2)$ satisfying these criteria is

$$v(q^2) = (4\pi)^{-1/2}q^2(q^2 + \alpha^2)^{-2}, \qquad (8)$$

where α^{-1} is the range of the force. Equation (8) is a simple generalization of the usual Yamaguchi form,[15] with the extra factor of $q^2(q^2 + \alpha^2)^{-1}$ playing the role of a potential barrier. (A similar form arises in the separable-potential treatment of a repulsive Coulomb force outside a nuclear attraction.[16]) It is, of course, this barrier that traps the particles into S wave resonances. For convenience we let α^{-1} be the unit of length from now on. We also put $h = M_H = 1$. With the form for v given in Eq. (8) and these units, Eq. (7) becomes

$$\tau(k^2) = -\left[\frac{\pi}{32\nu}\left(1 - \frac{16i\nu k^5}{(k^2+1)^4} \right.\right.$$
$$\left.\left. - \frac{\nu(1 + 5k^2 + 15k^4 - 5k^6)}{(k^2+1)^4} \right) \right]^{-1}, \qquad (9)$$

[13] L. D. Faddeev, *Mathematical Aspects of the Three-Body Problem in the Quantum Scattering Theory* (Israel Program for Scientific Translations, Jerusalem, 1965).

[14] See, e.g., J. V. Noble, Phys. Rev. **157**, 939 (1967), Appendix C.
[15] Y. Yamaguchi, Phys. Rev. **95**, 1628 (1954).
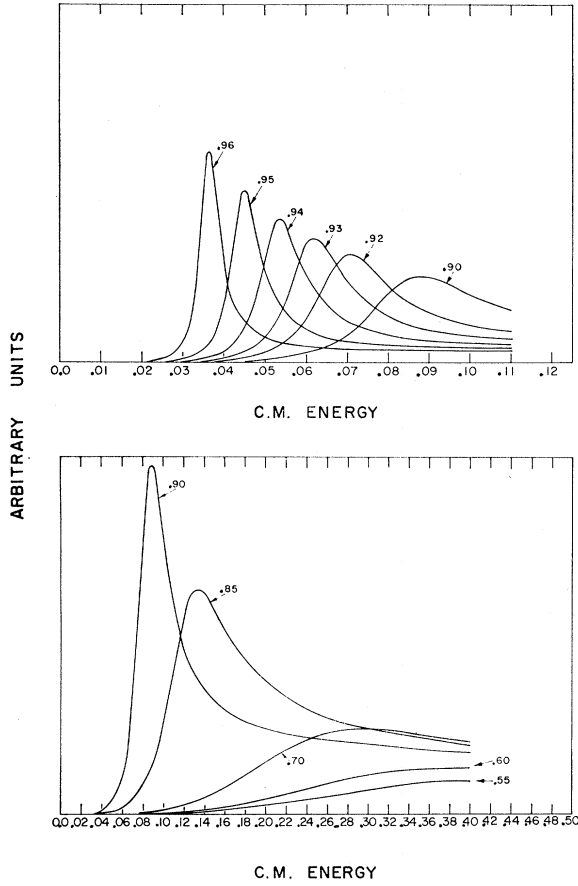[16] D. R. Harrington, Phys. Rev. **147**, 685 (1966).

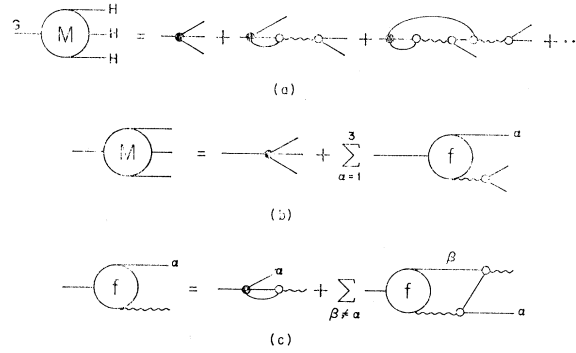FIG. 2. H-H cross sections as a function of energy, for values of ν as indicated.

FIG. 3. (a) Diagrammatic representation of the multiple scattering expansion for $G \to 3H$ weak decay. (b) Diagrammatic definition of f, the amplitude for decay of the G into H plus correlated H-H pair. (c) Diagrammatic representation of the off-shell integral equation for f.

where we have redefined the coupling constant $\lambda = 32\nu/\pi$ so that $\nu = 1$ corresponds to a zero-energy two-body bound state and $\nu = 0$ to no interaction. The H-H phase shifts for various values of ν over the energy range relevant to our three-body calculation are shown in Fig. 1. We see that for $\nu \sim 0.7$, the phase shift is large but nonresonant over a wide range of energies, whereas for $\nu \gtrsim 0.9$ there is a sharp low-energy H-H resonance. As $\nu \to 1$, the resonance energy goes to zero and the width vanishes. The phase shifts all start out with zero slope, since $v(0) = 0$. This means, of course, that the H-H scattering length is zero, and reflects the nonmonotonic nature of the interaction. The H-H cross section in the resonance region for various values of ν is shown in Fig. 2 for later comparison with the singles spectra from G decay.

C. Method of Solution of Three-Body Equations

The separable form of the two-body t matrix, Eq. (6), allows one to write the matrix element of Eq. (5) in the factored form

$$\langle \mathbf{p,q} | X(E)G_0(E)\mathfrak{IC}_{\text{weak}} | G \rangle$$
$$= v(q^2)\tau(E - \tfrac{3}{4}p^2)f(p^2,E). \quad (10)$$

The function $f(p^2,E)$ satisfies the reduced Faddeev equation

$$f(p^2,E) = g(p^2,E) + \int_0^\infty dp' p'^2 K(p,p'\,;E)f(p'^2,E), \quad (11)$$

where the kernel is given by

$$K(p,p'\,;E) = \lim_{\epsilon \to 0} 4\pi \int_{-1}^1 dt [v(p^2 + \tfrac{1}{4}p'^2 + pp't)$$

$$\times v(p'^2 + \tfrac{1}{4}p^2 + pp't)(E + i\epsilon - p^2 - p'^2 - pp't)^{-1}] \quad (12)$$

and where the inhomogeneous term $g(p^2,E)$ may be expressed in terms of the primitive weak-decay amplitude $\langle \mathbf{p,q} | \mathfrak{IC}_{\text{weak}} | G \rangle$ by

$$g(p^2,E) = \int d\mathbf{q}\, v(q^2)(E + i\epsilon - \tfrac{3}{4}p^2 - q^2)^{-1}$$

$$\times \langle \mathbf{p,q} | \mathfrak{IC}_{\text{weak}} | G \rangle. \quad (13)$$

The development of this sequence of equations for the weak-decay amplitude is represented diagrammatically in Fig. 3.

We now specify a form for the primitive weak decay amplitude appearing in Eq. (13). Since $q_\alpha^2 + \tfrac{3}{4}p_\alpha^2 = \sum_\beta \tfrac{1}{2}p_\beta^2$ is invariant under permutations of particle labels, as well as under coordinate rotations, it is convenient to take

$$\langle \mathbf{p,q} | \mathfrak{IC}_{\text{weak}} | G \rangle = \beta^2(\beta^2 + q^2 + \tfrac{3}{4}p^2)^{-1}. \quad (14)$$

From a computational point of view, this form was the simplest of several alternatives we considered. The spatial extension of the primitive weak vertex is determined by β^{-1} (in units of the strong-interaction range).

All quantities appearing in the integral equation (11) are now completely defined and it remains only to solve it. We do this by replacing the integrals by sums using Gaussian quadratures and inverting the resulting matrix equations on a high-speed computer. The singularities of the kernel were avoided by the contour-
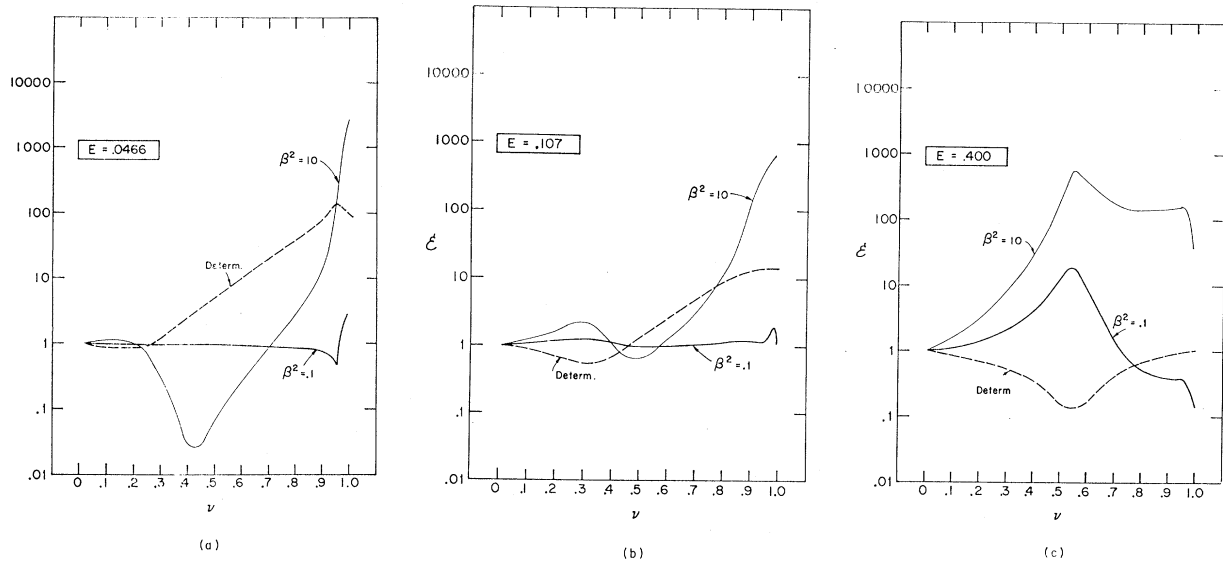
FIG. 4. The enhancements in $G \to 3H$ decay as a function of the H-H coupling strength ν for weak decay vertex ranges $\beta^2 = 10$ and $\beta^2 = 0.1$. Also shown (dashed curves) is the absolute value for the three-body Fredholm determinant. These are shown for kinetic-energy release of 0.0466 (a), 0.107 (b), and 0.400 (c).

deformation procedure introduced in these problems by Hetherington and Schick[17] and generalized to breakup reactions by Aaron *et al.*[3]

III. RESULTS

The partial decay rate of the G into 3 H's is a function of only two independent variables, because of the constraints of energy, angular momentum, and linear momentum conservation. We study the decay in the G rest frame and choose the two variables to be E_1 and E_2, the kinetic energies of two of the H particles. Combining these constraints with the requirements of Bose symmetry, we obtain in terms of the functions f, v, and τ defined in Sec. II, the following expression for the partial decay rate:

$$\mathfrak{R} \equiv \partial^2 R / \partial E_1 \partial E_2 = N \theta (E_1 E_2 - (\tfrac{1}{2}E - E_1 - E_2)^2)$$
$$\times |\beta^2 / (\beta^2 + E) + v(E - \tfrac{3}{2}E_1)\tau(E - \tfrac{3}{2}E_1) f(2E_1, E)$$
$$+ v(E - \tfrac{3}{2}E_2)\tau(E - \tfrac{3}{2}E_2) f(2E_2, E)$$
$$+ v(\tfrac{3}{2}E_1 + \tfrac{3}{2}E_2 - \tfrac{1}{2}E)\tau(\tfrac{3}{2}E_1 + \tfrac{3}{2}E_2 - \tfrac{1}{2}E)$$
$$\times f(2E - 2E_1 - 2E_2, E)|^2. \quad (15)$$

The constant N contains purely numerical factors (including the weak decay coupling constant which we have thus far suppressed, since the rate is simply quadratic in it). The theta function expresses the kinematic constraints. From Eq. (15), we have generated Dalitz plots and, by integrating once and twice, singles spectra and total rates, respectively. These are also the quantities most often extracted from experimental studies of three-body decays. We turn now to a detailed discussion of these quantities in our model.

[17] J. H. Hetherington and L. H. Schick, Phys. Rev. **137**, B935 (1965).

A. Total Rates

We are interested only in the dependence of the decay rates on the strong coupling constant ν and the weak-vertex structure parameter β^2.[12] In order to remove the trivial dependence on the weak coupling constant through N, and on the three-body phase space through the total energy E, we study the enhancement. This is defined in the usual manner by

$$\mathcal{E}(\nu, E, \beta^2) = \int dE_1 dE_2 \mathfrak{R}(\nu, E, \beta^2; E_1, E_2) \bigg/$$
$$\int dE_1 dE_2 \mathfrak{R}(0, E, \beta^2; E_1, E_2). \quad (16)$$

That is, the enhancement is the total decay rate normalized to the total rate in the absence of strong interactions. We have studied this enhancement for two values of β^2 (0.1 and 10), three values of the kinetic-energy release (0.0466, 0.107, and 0.400), and many values of ν between 0 and 1. When $\beta^2 = 0.1$, the weak vertex is spread out in configuration space compared with the range of the strong interaction. Conversely, $\beta^2 = 10$ corresponds to a nearly point vertex. The energies 0.0466 and 0.107 were chosen so that when it is kinematically allowed for two pairs of H's to resonate simultaneously, the corresponding pair-resonance widths would be, respectively, small or large in relation to their energies. The third value, $E = 0.4$, was chosen to favor the strong but nonresonant interactions occurring at $\nu \lesssim 0.75$. In Fig. 4(a) we have plotted the enhancement as a function of ν for $E = 0.0466$ and the two values of β^2. There is a striking difference between the enhancements corresponding to $\beta^2 = 10$ and $\beta^2 = 0.1$. From Eq. (1) we see

that when $\beta^2 = 10$, the decay rate is sensitive to the three-body wave function at small distances, while for $\beta^2 = 0.1$ the decay rate samples a large volume of the wave function. Clearly the strong interactions can (and do) affect the wave function ψ_{3H} at a point more than they can alter its average value taken over a large volume. For $\beta^2 = 10$ the enhancement varies over five orders of magnitude, from a de-enhancement of less than 0.03 to a maximum of 2500. We emphasize that this surprisingly large range of $\mathcal{E}$, including as it does substantial *de-enhancements*, results from a purely attractive *H-H* interaction of only moderate strength. The numerical origin of the de-enhancement around $\nu = 0.4$ is a nearly total cancellation between the direct breakup amplitude and the rescattering terms. The physical meaning of the de-enhancement eludes us. We see from Fig. 1 that as ν increases, the *H-H* subsystems can resonate. For $E = 0.0466$, *H-H* resonances are kinematically allowed only when $\nu \geq 0.94$. These resonances are quite narrow. When $\nu = 0.97$, all three pairs can resonate simultaneously. We see from Fig. 4(a) that there are no anomalies in the enhancements either at resonance production threshold or at the triple point. Previous authors have suggested that these may be singular points on the basis of perturbation theory.[18] However, other model calculations[6,7] as well as general arguments[6,8] support our conclusion that nothing special happens at these points. The very large enhancement for $\beta^2 = 10$ and $\nu \geq 0.95$ come entirely from the rescattering terms in the amplitude. By a numerical accident these terms have nearly the same magnitude as the first rescattering correction (impulse approximation). However, one should not regard this result as evidence for the validity of the many calculations using the impulse approximation: One need only turn to the results in Fig. 4(a) to
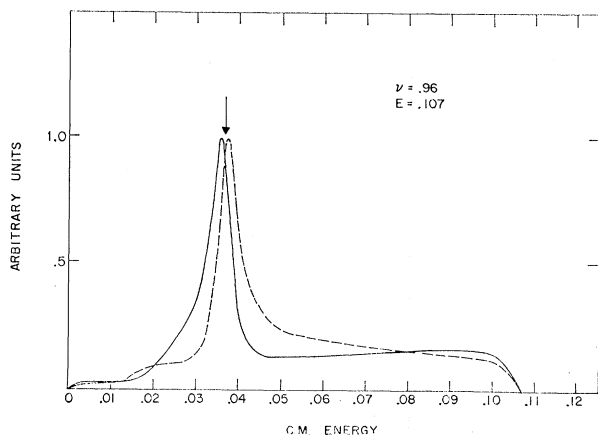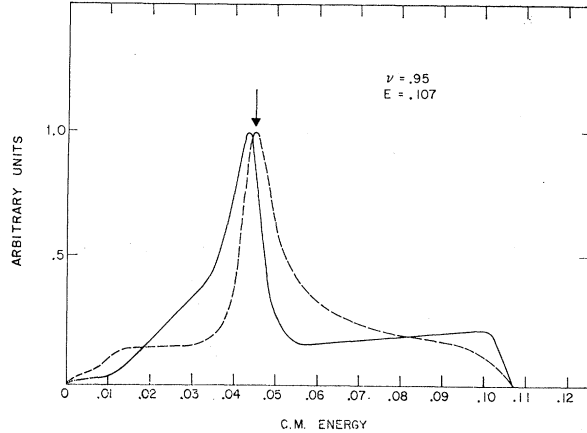

FIG. 6. Singles spectra for $G \rightarrow 3H$ decay as a function of the unobserved-pair relative energy ("missing mass") for $E = 0.107$, $\nu = 0.95$, $\beta^2 = 0.1$ (solid), and $\beta^2 = 10$ (dashed). The arrow indicates the input resonance position.

see the danger of this sort of a conclusion. The enhancements with $\beta^2 = 0.1$ are all very small and there is even a de-enhancement in the resonance region. The strong interactions for both cases are *identical* and the entire difference has come from the size of the primitive weak-interaction volume. Since β^2 enters only the inhomogeneous term of Eq. (11), and not the kernel, the convergence properties of the multiple scattering expansion are independent of it.

The enhancements for $E = 0.107$ and $E = 0.4$ appear in Figs. 4(b) and 4(c), respectively. Again we note a marked difference between $\beta^2 = 10$ and $\beta^2 = 0.1$. For $E = 0.107$ the resonances enter the kinematically allowed region around $\nu = 0.78$ although at this value of ν the *H-H* resonance is very broad. As ν approaches unity and the resonance energies approach zero, the diminishing three-body phase space causes the enhancement to decrease; which accounts for the drop in $\mathcal{E}$ near $\nu = 1$ in Figs. 4(b) and 4(c), since the f's vary imperceptibly there. This diminution of $\mathcal{E}$ is also present at $E = 0.0466$ but occurs too close to $\nu = 1$ to appear in Fig. 4(a).

Also plotted in Fig. 4 is the absolute value of the Fredholm determinant of the integral equation (11). As noted above, the determinant depends only on E and ν (and not on β^2). For each value of E, the determinant has a minimum in ν, corresponding to a three-body resonance in the sense that the real part of the determinant changes sign at the minimum. For computational reasons we have studied the variation of the determinant with ν, for fixed E. Clearly the variation with E for fixed ν parallels this; in particular the resonance becomes *narrower* and moves to *higher* energy as ν, the strength of the two-body interaction, increases. This behavior may seem contrary to intuition, but there is no reason to believe that all resonances are the analytic continuation of bound states to weaker coupling. In fact, there *is* a three-body bound state in
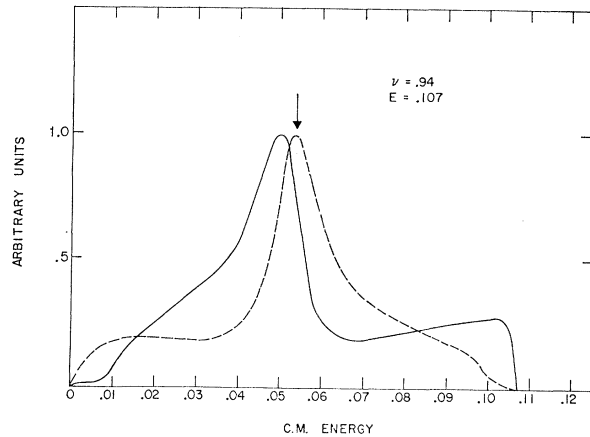

FIG. 5. Singles spectra for $G \rightarrow 3H$ decay as a function of the unobserved-pair relative energy ("missing mass") for $E = 0.107$, $\nu = 0.96$, $\beta^2 = 0.1$ (solid), and $\beta^2 = 10$ (dashed). The arrow indicates the input resonance position.

[18] R. F. Peierls, Phys. Rev. Letters **6**, 641 (1961); M. Month, Phys. Letters **18**, 357 (1965); I. J. R. Aitchison and C. Kacser, Phys. Rev. **142**, 1104 (1966).

FIG. 7. Singles spectra for $G \to 3H$ decay as a function of the unobserved-pair relative energy ("missing mass") for $E=0.107$, $\nu=0.94$, $\beta^2=0.1$ (solid), and $\beta^2=10$ (dashed). The arrow indicates the input resonance position.

our model which is unrelated to this resonance and whose binding energy can be shown to increase with ν. Since the energy analyticity of the determinant and its asymptotic limit of unity together imply that a bound-state zero gives rise to an anti-bound-state zero in the continuum, the question might arise as to whether the minimun of the determinant shown in Fig. 4 reflects the existence of a three-body bound state. The answer is that it does not. Such anti-bound states have no connection with the resonance discussed above, since the Hall-Post theorem[19] proves that there can be no three-body bound state and thus no anti-bound zero when ν is less than $\frac{2}{3}$, whereas in Fig. 4(c), for example, the resonance is at $\nu=0.55$.

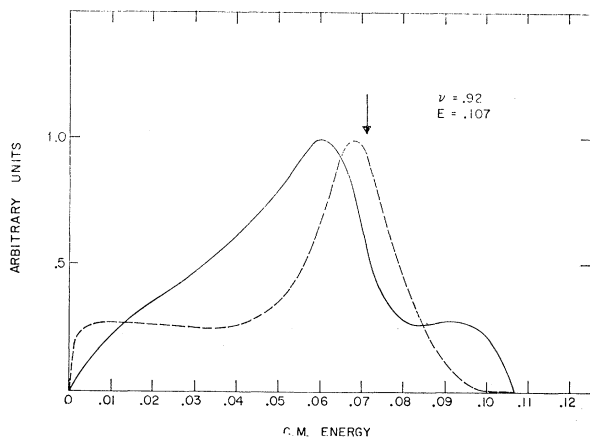The effect of the $3H$ resonance on the enhancement is twofold: It produces a local maximum in $\mathcal{E}$ (as a

FIG. 8. Singles spectra for $G \to 3H$ decay as a function of the unobserved-pair relative energy ("missing mass") for $E=0.107$, $\nu=0.92$, $\beta^2=0.1$ (solid), and $\beta^2=10$ (dashed). The arrow indicates the input resonance position.

[19] R. L. Hall and H. R. Post, Proc. Phys. Soc. (London) **90**, 38 (1967).

function of ν), and the change in sign of the real part of the determinant produces a corresponding sign change in the real part of f [defined by Eq. (11)]. As we see in Eq. (15), this sign change accounts for the interference minimum in $\mathcal{E}$ occurring at ν slightly above ν(resonance). Whether the resonance maximum, or the interference minimum, or the final-rescattering enhancement, is the most striking feature of $\mathcal{E}$ as a function of ν depends on the detailed behavior of all the amplitudes involved. The only general feature that we can extract from Fig. 4 is that enhancements and de-enhancements of several orders of magnitude accompany a relatively compact primitive weak vertex, whereas no striking effect on the rate occurs in the case of a spread out vertex. Except for this restriction, virtually any value of the enhancement can be obtained by a reasonable choice of parameters.

B. Single-Particle Spectra

Integrating the double-differential rate of Eq. (15) over one of the energies gives the single-particle (singles) spectrum, dR/dE_1. This is the probability for G decay with one H having energy E_1. Because of the

TABLE I. Ratios of extracted (expt) to input (res) resonance parameters for $E=0.107$.

ν	$\beta^2=0.1$		$\beta^2=10$	
	E_{expt}/E_{res}	$\Gamma_{expt}/\Gamma_{res}$	E_{expt}/E_{res}	$\Gamma_{expt}/\Gamma_{res}$
0.96	0.97	1.00	1.01	1.0
0.95	0.97	1.00	1.00	1.0
0.94	0.93	1.15	0.99	1.0
0.92	0.86	1.35	0.97	0.76
0.90	0.77	0.95	0.85	0.55

constraints of energy and momentum conservation, the energy of particle 1 in the total c.m. system is related to the relative energy of particles 2 and 3 in their own c.m. system. The relation is

$$\tfrac{3}{2}E_1 + E_{23} = E. \qquad (17)$$

Thus the independent variable in the singles spectra may be chosen as the relative H-H energy. This is the nonrelativistic analog of the invariant pair mass usually chosen as the variable in relativistic multibody reactions. We expect, therefore, that the singles spectra, as a function of the relative H-H energy, will reflect the H-H interaction and in particular the two-body resonance. The interesting question is to what extent will the resonance parameters—position, width, shape—in the singles spectra accurately reflect the two-body data, and to what extent does this depend on the reaction mechanism. That is, how reliably can one extract the two-body information from the behavior of the three-body final state? Figures 5–9 exhibit the singles spectra for $E=0.107$ and various values of ν in the resonance region, for both values of β^2, all normalized to the same height. From Fig. 4(b) we see that in this range of ν

the rates corresponding to $\beta^2 = 10$ are more than 100 times larger than those for $\beta^2 = 0.1$. The H-H resonance clearly dominates the spectrum in each case, but the effects of three-body phase space (see Fig. 12) and interference between the resonant and nonresonant parts of the amplitude considerably modify the simple resonance curves of Fig. 2. We have extracted the position and width of the H-H resonance from the singles spectra in a rather crude fashion: We subtracted a constant background and then read off the position of the maximum, and the width, graphically. Although more sophisticated procedures are generally used to analyze experiments,[20] there is no reason to regard them as having a more fundamental theoretical justification. In particular, there is no reason to believe that phase space is a multiplicative factor that can therefore be divided out. The parameters we extracted are compared in Table I with the two-body parameters similarly extracted from Fig. 2. (We have made no attempt to fit any resonance with a Breit-Wigner formula, since
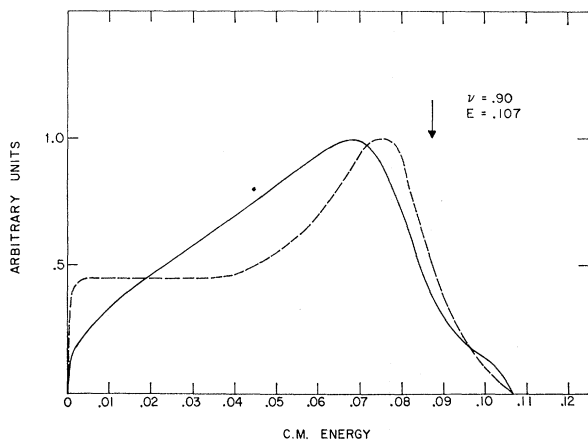

Fig. 9. Singles spectra for $G \rightarrow 3H$ decay as a function of the unobserved-pair relative energy ("missing mass") for $E = 0.107$, $\nu = 0.90$, $\beta^2 = 0.1$ (solid), and $\beta^2 = 10$ (dashed). The arrow indicates the input resonance position.

it is unnecessary for the narrow resonances, and inappropriate for the broad asymmetric ones.) For $\nu = 0.96$ and 0.95, the resonances are quite narrow compared with their own position and also with E, the energy released in the decay. Hence the resonance parameters are quite accurate in these cases. Nevertheless, the effects of interference, important for $\beta^2 = 0.1$, considerably alter the resonance shape, as we see in Figs. 5 and 6. As ν increases, and the resonances broaden and move higher in energy, the quality of the extracted parameters deteriorates. For $\nu = 0.94$, the $\beta^2 = 0.1$ parameters are somewhat off, despite the fact that the resonance is still fairly narrow and near the center of the spectrum. Presumably this is an effect of the interference. For

[20] P. Anninos, L. Gray, P. Hagerty, T. Kalogeropoulos, S. Zenone, R. Bizzarri, G. Ciapetti, M. Gaspero, I. Laakso, S. Lichtman, and G. C. Moneti, Phys. Rev. Letters **20**, 402 (1968).
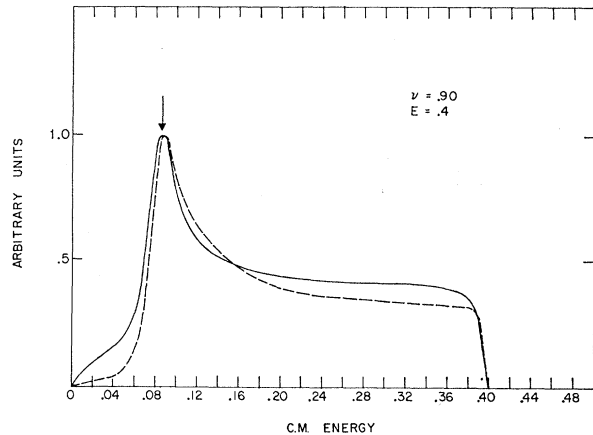

Fig. 10. Singles spectra for $G \rightarrow 3H$ decay as a function of the unobserved-pair relative energy ("missing mass") for $E = 0.4$, $\nu = 0.90$, $\beta^2 = 0.1$ (solid), and $\beta^2 = 10$ (dashed). The arrow indicates the input resonance position.

$\nu = 0.92$ and 0.90, the parameters are adversely affected both by interference and by the proximity of the kinematical boundary. Interference in the $\beta^2 = 0.1$ curves tends to broaden the resonance by giving it a low-energy shoulder. The kinematical boundary tends to narrow the resonance and push it to lower energies by suppressing the high-energy tail, which, as we see from Fig. 2, is particularly important for these values of ν. The competition of these effects can be seen in the behavior of the width ratio for $\beta^2 = 0.1$, as a function of ν.

In Figs. 10 and 11 we show the singles spectra for $E = 0.4$ and for $\nu = 0.90$ and 0.85, for both values of β^2, normalized to the same height. From Fig. 4(c) we see that there is a factor of over 100 between the $\beta^2 = 10$ and $\beta^2 = 0.1$ rates for these values of ν. Once more, the two-body H-H resonance dominates the spectrum, as can be seen from comparing Figs. 10 and 11 with Fig. 2.
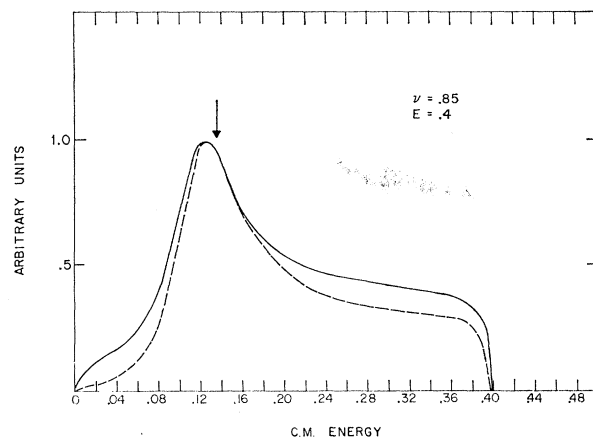

Fig. 11. Singles spectra for $G \rightarrow 3H$ decay as a function of the unobserved-pair relative energy ("missing mass") for $E = 0.4$, $\nu = 0.85$, $\beta^2 = 0.1$ (solid), and $\beta^2 = 10$ (dashed). The arrow indicates the input resonance position.
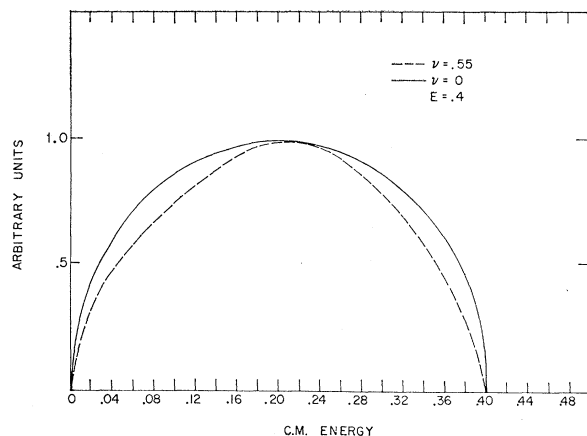
FIG. 12. Singles spectrum for $E=0.4$ and $\nu=0.55$ (dashed curve, both values of β^2) compared with phase space ($\nu=0$, solid curve).

The resonance parameters have been extracted from these spectra by the method described above and are compared with the two-body parameters in Table II. For $\nu=0.90$ they are not bad, but for $\nu=0.85$ the width in particular is far too small for both values of β. What is perhaps most surprising is that the resonance comes at too *low* an energy in spite of the proximity of the low-energy kinematical boundary which might be expected to push the energy up, not down. Since this effect occurs for the higher-energy resonance at $\nu=0.85$ and not for $\nu=0.90$, it must be of dynamical origin and is presumably related to the asymmetric form of the resonance and its long high-energy tail; that is, to the fact that for $\nu=0.85$ the phase shift does not get very far above 90° before it turns over. The detailed connection between this feature of the two-body amplitude and the singles spectrum is, of course, not clear.
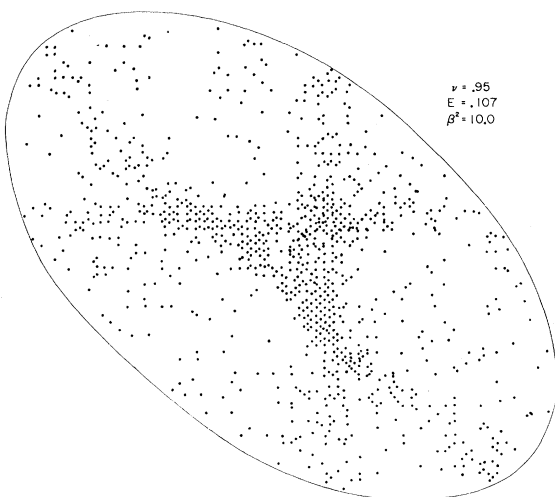

FIG. 13. Dalitz plot for $G \rightarrow 3H$ decay, $E=0.107$, $\beta^2=10$, and $\nu=0.95$. The ordinate and abscissa are E_1 and E_2, the kinetic energies of any two H particles.

In Fig. 12 we show the singles spectrum for $\nu=0.55$ and for $\nu=0$. The shapes for $\beta^2=10$ and 0.1 are indistinguishable for $\nu=0.55$. The value $\nu=0$, of course, gives just phase space. From Fig. 4(c), we see that $\nu=0.55$ corresponds to the peak of the enhancements, nearly 1000 for $\beta^2=10$ and over 10 for $\beta^2=0.1$, whereas from Fig. 3(b) we see that $\nu=0.55$ corresponds to a very modest two-body interaction. In spite of these enormous enhancements, the $\nu=0.55$ spectrum is nearly identical with the phase-space distribution. In fact the difference is exaggerated by our normalization to the same height: Had we normalized to the same *area*, the maximum discrepancy would never exceed 7%. The moral is clear: Neither a spectrum spanlike phase space nor a relatively weak two-body force is sufficient reason to trust the Born approximation.

In summary, we emphasize several points. The phenomenological extraction of two-body resonance parameters from singles spectra can be misleading. If the resonances are narrow and far from the limits of phase space, the extraction of parameters is relatively reliable, although even here there is considerable mechanism dependence. In our particular model the results were better for small interaction volume ($\beta^2=10$); this

TABLE II. Ratios of extracted (expt) to input (res) resonance parameters for $E=0.4$.

| ν | $\beta^2=0.1$ | | $\beta^2=10$ | |
	E_{expt}/E_{res}	$\Gamma_{expt}/\Gamma_{res}$	E_{expt}/E_{res}	$\Gamma_{expt}/\Gamma_{res}$
0.90	1.0	0.80	1.0	1.0
0.85	0.93	0.64	0.93	0.64

agrees with the original physical treatment of final-state interactions by Watson, Migdal, and Fermi.[1] Moreover, we see from Tables I and II that there is no systematic trend in the deviations. The widths especially can be either narrowed or broadened by three-body effects.

Finally, we note that strong enhancements can be produced by rather weak H-H interactions, leading to a singles spectrum hardly distinguishable from phase space.

C. Dalitz Plots

We simulated "experimental" Dalitz plots from the rate function $\mathfrak{R}$ of Eq. (15) on a high-speed computer, by using an appropriate psuedo-random-number generator. Some typical plots with $E=0.107$ and $\nu=0.95$ and 0.92 for each value of β^2 are shown in Figs. 13–16. E_1 and E_2, the kinetic energies of two of the particles, are measured along the horizontal and vertical axes. These are the independent variables of Eq. (15). As usual, the density of points per unit area is proportional (within statistics) to the doubly differentiated decay rate, Eq. (15). A constant decay probability thus leads to a uniform density of points within the kinematically

allowed region. The E_1 and E_2 scales are not precisely equal, since we generated these plots on the fast printer of the computer. The relative coarseness of the grid in some of the plots also results from this method of constructing them.

From Fig. 4(b) we see that the enhancement for $\nu=0.95$ is very large for $\beta^2=10$ and of the order of unity for $\beta^2=0.1$. The extracted resonance parameters in this case (Table I) are good, but the singles spectra (Fig. 6) show the effects wrought by interference when $\beta^2=0.1$. The Dalitz plots for $\nu=0.95$ appear in Figs. 13 and 14. When $\beta^2=10$ (Fig. 13) the resonance bands stand out quite clearly, as we would expect from the enhancements and singles spectrum. The decay amplitude is here completely dominated by the three terms containing the final H-H resonances. Recall that as one crosses a resonance band, the phase of the corresponding term of the amplitude changes by π. Hence at the
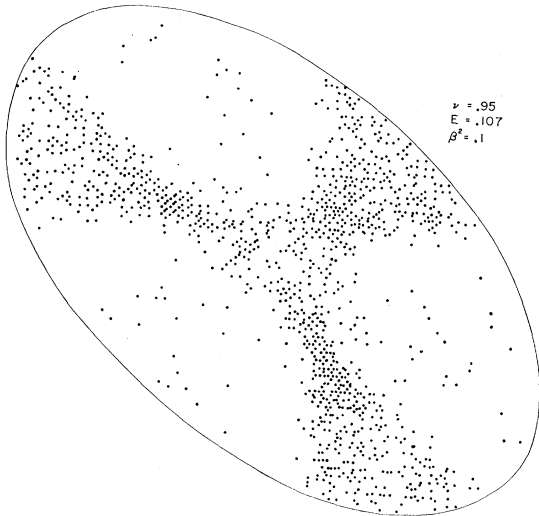

Fig. 15. Dalitz plot for $G \rightarrow 3H$ decay, $E=0.107$, $\beta^2=10$, and $\nu=0.92$. The ordinate and abscissa are E_1 and E_2, the kinetic energies of any two H particles.

We emphasize once more that the strong interactions are identical in these two cases. Instead of well-defined resonance bands we find an intriguing trefoil pattern in Fig. 14. The regions of increased point density represent constructive interference between adjacent resonance bands and the bare amplitude, whereas the depleted regions result from destructive interference. The regions alternate because of the phase change across the resonance bands. There is also a region of depletion in the center. These regions of depletion superficially resemble those predicted by simple kinematical considerations, for a G particle of higher spin; however, detailed comparison with these predictions reveals that no

Fig. 14. Dalitz plot for $G \rightarrow 3H$ decay, $E=0.107$, $\beta^2=0.1$, and $\nu=0.95$. The ordinate and abscissa are E_1 and E_2, the kinetic energies of any two H particles.

crossing of two (or even three) bands the average of the interference term, taken over the crossing region, is zero. The average point density at a two-band crossing is twice that in a single band. If all three cross, the factor is 3. Therefore the over-all enhancement shows no anomalies when bands cross, as we noted in Sec. III A. Although its average is zero, the two-band interference term does produce local maxima and minima in the crossing region. When $\beta^2=0.1$ (Fig. 14), the re-scattering corrections are such that the resonance terms no longer dominate the amplitude, but have the same order of magnitude as the bare decay amplitude, and hence interfere with it, as well as with each other. The effects of this interference are evident in the striking difference between Fig. 14 ($\beta^2=0.1$) and Fig. 13 ($\beta^2=10$).
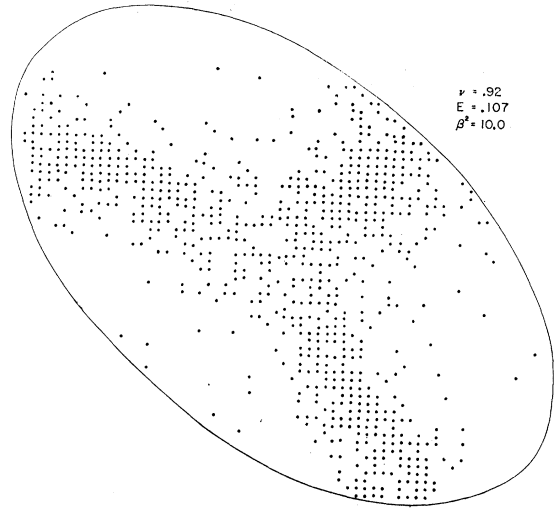

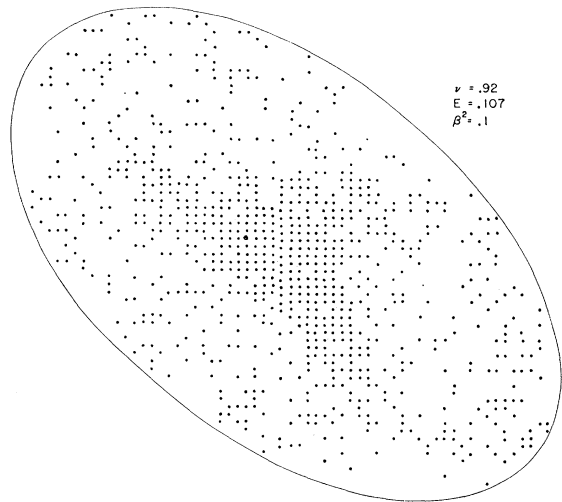
Fig. 16. Dalitz plot for $G \rightarrow 3H$ decay, $E=0.107$, $\beta^2=0.1$, and $\nu=0.92$. The ordinate and abscissa are E_1 and E_2, the kinetic energies of any two H particles.

higher spin-parity assignment is compatible with this pattern (Fig. 14).[21]

When $v=0.92$, the enhancements for the two values of β are quite different, the singles spectra (Fig. 8) are very different, and the resonance parameters (Table I) are poorly determined from them. These differences are reflected in the Dalitz plots, Figs. 15 and 16. A semblance of band structure remains in Fig. 15 ($\beta^2=10$), but none is apparent in Fig. 16. The clustering of points toward the center of the Dalitz plot for $\beta^2=0.1$ (Fig. 16) indicates a strong preference for states with equally distributed momentum. If one did not know otherwise, this might suggest repulsive pairwise interactions; of course, it is actually an effect of interference. Once again, from detailed comparison with kinematical predictions, we find that Fig. 16, while suggestive, is not compatible with higher spin for the G. None of our computer-generated Dalitz plots has depletions which could be mistaken for a different spin assignment for the G. However, it is conceivable that dynamical effects similar to those studied here could mislead by simulating incorrect spin patterns.

Part of the distribution of dots in our Dalitz plots is due to the variation of the function f appearing in Eq. (15). The real and imaginary parts of this quantity typically vary by a factor of 3, over the physical energy range. In the case of resonance dominance (Figs. 13 and 15, $\beta^2=10$), this variation is slow enough to be neglected. However, when $\beta^2=0.1$, the effect is important and precludes the phenomenological representation of the amplitude by a sum of Breit-Wigner terms plus a constant. Clearly the important role of interference makes the representation of the rate by the incoherent sum of the squares of Breit-Wigner amplitudes plus a background even less appropriate.

IV. SUMMARY, CONCLUSIONS, AND PROSPECTUS

We have explored an exactly soluble model of a weak three-body decay of a scalar parent (the G) into three scalar decay products (the H's), in order to study the effects of final-state interactions (FSI). Our model was designed to elucidate in a moderately realistic fashion situations in which overlapping resonances occur in the final state, while retaining sufficient simplicity to be exactly solvable. Even within such a relatively narrow framework, we find an alarming variety of dynamical effects.

We have examined the effects of FSI on total-rate enhancements, singles spectra, and Dalitz plots. We find that moderately strong attractive pairwise interactions can produce large (of order 10^3) enhancements and large (of order 10^{-2}) de-enhancements when the bare weak-decay amplitude is of short range, whereas when it is spread out, identical FSI produce virtually no enhancement or de-enhancement of the total rate.

Furthermore, we observe no anomalies in the total rate which could be attributed to resonant kinematical rescattering singularities.[18] We have examined the important question of how well two-body resonance parameters can be extracted from singles spectra. We find that for sharp resonances, well centered in phase space, this can be done fairly well, as expected. When the resonances are broad or near the limits of phase space, the extracted parameters are considerably less reliable, although the decays originating in a small weak-interaction volume provide better extracted parameters than those originating from a large volume. Surprisingly, there seem to be no obvious trends in the deviations from the true (input) parameters. For example, we find cases of resonance broadening as well as cases of narrowing in our singles spectra. All these results indicate that when the decay is characterized by a small weak-interaction volume, the final state is dominated by resonant rescattering. Hence the corresponding Dalitz plots show clear resonance bands and offer no ambiguities in their interpretation. Moreover, nothing unexpected happens when the resonance bands cross in the Dalitz plot. On the other hand, when the weak vertex is spread out, resonant rescattering terms no longer dominate the amplitude, but are comparable (even on resonance) with the bare weak-decay amplitude. There is thus considerable interference between all terms of the decay amplitude, and the Dalitz plots become correspondingly complicated and are difficult to interpret.

As is clear from the above resume, the one parameter with the greatest qualitative effect is the size of the bare weak-decay vertex. This parameter is the only one characterizing the production mechanism in our simple model. This sensitivity suggests that in more general reactions producing three-hadron final states, the production mechanism and the rescattering effects will be hard to disentangle, each profoundly affecting the other. We plan to investigate models involving strong production in order to learn more about these phenomena. We also hope to investigate the dependence of our results on some of the (admittedly arbitrary) simplifying assumptions we have made in order to keep the problem manageable.

It is somewhat reassuring to find a large dynamic range in rate enhancements resulting from moderately strong FSI: It is plausible that such puzzles as the anomalously rapid $\eta \rightarrow 3\pi$ decay or the unexpectedly slow $X^0 \rightarrow \eta\pi\pi$ rate could find their explanation in terms of FSI effects rather than by invoking esoteric symmetries or new conservation laws.[22] On the other hand, this same sensitivity to a variety of parameters precludes a meaningful calculation at our present level of knowledge.

[21] C. Zemach, Phys. Rev. **133**, B1201 (1964).

[22] We are aware, of course, that the $X^0 \rightarrow \eta\pi\pi$ decay is thought not to be a weak decay. This in no way modifies our conclusion on the importance of final rescattering in the enhancements. It would also not affect the shapes of spectra or Dalitz plots.

An interesting offshoot of our investigation was the discovery of a three-hadron resonance which has the unusual property of moving to higher energy and becoming more prominent as the H-H coupling is increased. Pagels[23] has suggested that there might exist a three-pion resonance just above 0.42 BeV/c^2, with the quantum numbers of the pion. Although the absence of isospin in our model makes detailed comparison impossible, the analogy is suggestive, particularly since our H-H interaction, for moderate strengths, produces a phase shift closely resembling current ideas about

the S-wave π-π interaction.[24] We are currently investigating the properties of this resonance in more detail.

ACKNOWLEDGMENTS

We would like to thank Professor S. Frankel, Professor S. P. Rosen, and Professor H. Primakoff for many valuable conversations.

[23] H. Pagels, Phys. Rev. **179**, 1337 (1969).

[24] That is, our phase shift resembles recent phenomenological analyses of the S-wave $T=0$ π-π phase shift [S. Marateck *et al.*, Phys. Rev. Letters **21**, 1613 (1968)]. It also has the small scattering length required by current algebra [S. Weinberg, Phys. Rev. Letters **17**, 616 (1966)].

Electromagnetic Simulation of Time-Reversal Violation in Mirror Spin-$\frac{3}{2}$ Beta Decays*

HERBERT H. CHEN†

Palmer Laboratory, Princeton University, Princeton, New Jersey 08540

(Received 14 April 1969)

With time-reversal invariance, the β-decay correlation $(\langle \mathbf{J}\rangle/J)\cdot\mathbf{p}_l\times\mathbf{p}_\nu$, where $\langle \mathbf{J}\rangle/J$ is the polarization of the decaying nucleus and $\mathbf{p}_l$ ($\mathbf{p}_\nu$) is the momentum of the electron (neutrino), can arise only through a final-state electromagnetic interaction. For allowed transitions with vector and axial-vector couplings, this effect is recoil-dependent. It was shown by Callan and Treiman that this effect, for the special class of spin-$\frac{1}{2}$ mirror transitions, and the assumption of the conserved-vector-current (CVC) hypothesis, is dominated by weak magnetism. A corresponding calculation for the class of spin-$\frac{3}{2}$ mirror transitions, of which the decay $\text{Ar}^{35}\rightarrow\text{Cl}^{35}+e^++\nu_e$ is an example, shows a similar domination by weak magnetism. The magnitude of this effect is estimated for several mirror β transitions.

INTRODUCTION

ONE of the classic tests of T invariance in nuclear β decay is the search for a possible correlation in the decay spectrum of the form $(\langle \mathbf{J}\rangle/J)\cdot(\mathbf{p}_l\times\mathbf{p}_\nu)$, where $\langle \mathbf{J}\rangle/J$ is the polarization of the decaying nucleus, and $\mathbf{p}_l$ ($\mathbf{p}_\nu$) is the momentum of the electron (neutrino). In the absence of electromagnetic final-state interactions, this correlation is forbidden by time-reversal invariance. Experimental upper limits on the presence of such a correlation term have been obtained for the spin-$\frac{1}{2}$ mirror transitions $n \rightarrow pe\bar{\nu}$ [1] and $\text{Ne}^{19} \rightarrow \text{F}^{19}e^+\nu$.[2] There is also possible experimental interest on this correlation in the spin-$\frac{3}{2}$ mirror transition $\text{Ar}^{35} \rightarrow \text{Cl}^{35}e^+\nu$.[3]

The allowed β spectrum, summed over all final-spin polarizations, has the following form in the standard

theory with vector and axial-vector couplings (with the neglect of nuclear recoil[4]):

$$d\omega(\langle \mathbf{J}\rangle \mid E_l,\Omega_l,\Omega_\nu)\, dE_l d\Omega_l d\Omega_\nu$$

$$=\frac{F(\mp Z,E_l)}{(2\pi)^5}p_l E_l(E_0-E_l)^2 dE_l d\Omega_l d\Omega_\nu\xi\left\{1+a\frac{\mathbf{p}_l\cdot\mathbf{p}_\nu}{E_l E_\nu}\right.$$

$$+c\left[\frac{\mathbf{p}_l\cdot\mathbf{p}_\nu}{3E_l E_\nu}-\frac{(\mathbf{p}_l\cdot\hat{J})(\mathbf{p}_\nu\cdot\hat{J})}{E_l E_\nu}\right]\left[\frac{J(J+1)-3(\mathbf{J}\cdot\hat{J})^2}{J(2J-1)}\right]$$

$$\left.+\frac{\langle \mathbf{J}\rangle}{J}\cdot\left[A\frac{\mathbf{p}_l}{E_l}+B\frac{\mathbf{p}_\nu}{E_\nu}+D\frac{\mathbf{p}_l\times\mathbf{p}_l}{E_l E_\nu}\right]\right\}, \quad (1)$$

where $F(\mp Z,E_l)$ is the well-known Fermi function that accounts for the Coulomb modification of the electron (positron) spectrum; ξ, a, c, A, B, and D are simply related to the vector and axial-vector couplings which are, effectively, constants in the realm of β decay; and $\hat{J}$ is a unit vector along $\mathbf{J}$. Present experimental limits on D, the coefficient of the correlation effect $(\langle \mathbf{J}\rangle/J)$

[1] M. T. Burgy, V. E. Krohn, T. B. Novey, G. R. Ringo, and V. L. Telegdi, Phys. Rev. **120**, 1829 (1960); M. A. Clark and J. M. Robson, Can. J. Phys. **38**, 693 (1960); B. G. Erozolimsky, L. N. Bondarenko, Yu A. Mostovoy, B. A. Obinyakov, V. P. Zacharova, and V. A. Titov, Phys. Letters **27B**, 557 (1968).

[2] F. P. Calaprice, E. D. Commins, H. M. Gibbs, and G. L. Wick, Phys. Rev. Letters **18**, 918 (1967).

[3] E. D. Commins (private communication via S. B. Treiman).

[4] J. D. Jackson, S. B. Treiman, and H. W. Wyld, Jr., Nucl. Phys. **4**, 206 (1957); see also Phys. Rev. **106**, 517 (1957).